

Corrosion Inhibition Effect of D-sodium Gluconate on Reinforcing Steel in Chloride-contaminated Simulated Concrete Pore Solution

Jian-Hua Li¹, Bing Zhao¹, Juan Hu¹, Hui Zhang¹, Shi-Gang Dong², Rong-Gui Du^{1,*} and Chang-Jian Lin¹

¹ Department of Chemistry, College of Chemistry and Chemical Engineering, Xiamen University, Xiamen, Fujian 361005, P. R. China

² School of Energy Research, Xiamen University, Xiamen, Fujian 361005, P. R. China

*E-mail: rgdu@xmu.edu.cn

Received: 28 October 2014 / Accepted: 27 November 2014 / Published: 2 December 2014

The corrosion inhibition effect and mechanism of D-sodium gluconate for reinforcing steel in the simulated concrete pore solution containing Cl⁻ were studied by electrochemical techniques, including corrosion potential, potentiodynamic polarization, and electrochemical impedance spectroscopy measurements. The results indicate that 0.01 M D-sodium gluconate showed a good corrosion inhibition effect on reinforcing steel in the simulated concrete pore solution containing 0.1 M NaCl because it strongly hindered the anodic reactions. The inhibition mechanism could be explained on the basis of the competitive adsorption between gluconate anions and chloride ions on the reinforcing steel surface. And D-sodium gluconate could eventually form a compact adsorptive film by strong chelation and effectively inhibit the initiation of reinforcing steel corrosion.

Keywords: Reinforcing steel; Simulated concrete pore solution; Corrosion inhibitor; D-sodium gluconate; EIS

1. INTRODUCTION

Reinforcing steel corrosion is a major cause of premature degradation of concrete structures, and has been a serious and significant problem in modern society.

It is well known that reinforcing steel in concrete is normally protected against corrosion by the passive film formed on its surface under high alkaline conditions of concrete. However, the reinforcing steel corrosion may take place if the condition of passivation is destroyed by the presence of Cl⁻ and/or the carbonation of concrete, etc [1-4]. When the Cl⁻ concentration reaches a threshold value at the

steel/concrete interface, the Cl^- attack will cause local depassivation and pitting corrosion of the reinforcing steel [3-6]. The process of carbonation, leading to a pH decrease in the concrete pore solution, can also break down the passive film [2,3,7-9]. The development of the reinforcing steel corrosion can lead to the damage or even local ruin of the reinforced concrete structures due to the rust formation and/or loss in cross-section of the reinforcing steel.

Many techniques have been developed to prevent the corrosion of reinforcing steel in concrete, including the use of corrosion inhibitors [3, 10-14], cathodic protection [3, 15-17], electrochemical treatment [18-20], epoxy coated rebar [21,22] and galvanized rebar [23,24], etc. Among these available techniques, the use of corrosion inhibitors has been developed rapidly in the past twenty years, which is more attractive from the point of view of low cost and easy application.

Many compounds have been tested as corrosion inhibitors against the corrosion of reinforcing steel in concrete. For example, The nitrites, mainly calcium and sodium nitrites are mostly used as inorganic corrosion inhibitors [25-27], but they are toxic. Sodium monofluorophosphate are widely applied in carbonated and chloride-contaminated concrete [28-30]. Over the last decades, the use of organic inhibitors has been increased. The organic inhibitors mainly include aminoalcohol [31-33], amines, fatty-acid esters or their mixtures [34-37]. Although many organic inhibitors have been investigated, there are still many problems to be solved regarding their applications and inhibition effects.

There is an increasing demand for eco-friendly inhibitors for use in concrete. Gluconates and gluconic acid have been reported to be effective non-toxic inhibitors for iron and mild steel in cooling water systems [38-42]. Sodium gluconate can provide the complete protection of mild steel immersed in a weak alkaline media [43]. However, few studies can be found regarding the gluconate used as the inhibitor for reinforcing steel in concrete [34].

Electrochemical impedance spectroscopy (EIS) is widely used to study the corrosion inhibitors, which can provide the information about both the inhibitive efficiency and the inhibition mechanism of the investigated inhibitors [31,32,44,45].

The objective of this work is to study the electrochemical behavior of reinforcing steel in the simulated concrete pore solution (SPS) in the presence of Cl^- and the corrosion inhibition effect of D-sodium gluconate on the steel by electrochemical methods.

2. EXPERIMENTAL

The specimens ($\text{Ø}1.14 \text{ cm} \times 0.4 \text{ cm}$) were cut from a R235 reinforcing steel rod. After degreased and cleaned, each specimen was mounted with epoxy resin and only one cross section ($\text{Ø}1.14 \text{ cm}$) was exposed as working surface (approximately 1 cm^2). The working surface was polished successively with emery papers of grade from 400 to 1500, and then rinsed with de-ionized water. All solutions were prepared with de-ionized water and AR chemicals. The saturated $\text{Ca}(\text{OH})_2$ solution, used as the SPS, containing 0.1 M NaCl was employed to simulate the chloride-contaminated inner electrolytic medium of concrete. D-sodium gluconate with the concentration of 0.01 M was used as the corrosion inhibitor and added to the SPS containing 0.1 M NaCl.

Corrosion potential (E_{corr}), potentiodynamic polarization curve, and EIS measurements were all performed by Autolab Potentiostat Galvanostat (Eco Chemie, the Netherlands) with PGSTAT30. The potentiodynamic polarization curve and EIS measurements were all carried out in a three-electrode cell. The reinforcing steel was used as the working electrode, a platinum sheet as the counter electrode, and a saturated calomel electrode (SCE) as the reference electrode connected with the test cell by a salt bridge. The potentiodynamic polarization was conducted at a scan rate of 1 mV s^{-1} . The EIS measurements were made by the Autolab with PGSTAT30 and FRA module at the corrosion potential over a frequency range between 10^5 Hz and 10^{-2} Hz . The amplitude of the wave was 10 mV . The experimental impedance spectra were fitted to the equivalent circuit by the FRA software of Autolab. All the tests were carried out at room temperature ($25 \pm 2 \text{ }^\circ\text{C}$).

3. RESULTS AND DISCUSSION

3.1. Corrosion potential evolution

Figure 1 depicts the E_{corr} evolution of the reinforcing steel immersed in SPS containing 0.1 M NaCl without and with 0.01 M D-sodium gluconate. From Figure 1, it can be seen that the E_{corr} evolution was very different in the presence and absence of D-sodium gluconate. The E_{corr} values for the reinforcing steel in the SPS containing 0.1 M NaCl without the inhibitor decreased slowly during the first 36 h immersion, reaching low values about -0.520 V .

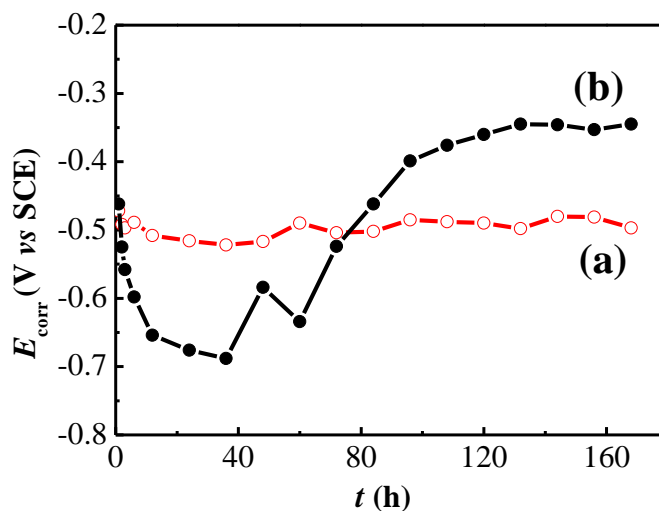


Figure 1. Evolution of the corrosion potential of reinforcing steel immersed in SPS containing 0.1 M NaCl (a) without and (b) with 0.01 M D-sodium gluconate.

This decay of E_{corr} suggested that Cl^- induced the initiation of corrosion. After that, the E_{corr} increased slowly with time and stabilized about -0.490 V after 60 h of immersion, related to the development and final severe corrosion of the reinforcing steel. At the very beginning of immersion,

the E_{corr} showed almost the same values with and without the inhibitor. However, with the addition of D-sodium gluconate, the E_{corr} declined sharply to very low values (about -0.690 V) during the initial 36 h of immersion. This decrease may be the result of the competitive adsorption between the chloride ions and the gluconate anions on the steel surface. Then, the E_{corr} shifted largely towards the positive direction and became higher than that without the inhibitor after about 84 h of immersion. After 132 h, the E_{corr} changed very little with time, attaining values about -0.350 V. The increase and then little change of the E_{corr} indicated that the adsorption of gluconate anions was becoming predominant and finally formed a compact adsorptive film on the steel surface.

3.2. Potentiodynamic polarization curves

Potentiodynamic polarization curves for the reinforcing steel in SPS containing 0.1 M NaCl without and with 0.01 M D-sodium gluconate are shown in Figure 2. Because the shift of the E_{corr} was not always towards one direction, potentiodynamic polarization curve measurements were carried out in the presence of D-sodium gluconate during different immersion times. It can be seen that, with the addition of D-sodium gluconate, both the anodic and cathodic currents of the reinforcing steel were inhibited. The decrease in the anodic currents was significant, while the decrease of the cathodic currents was rather slight, showing the anodic polarization was more significant than the cathodic polarization. These results suggested that the anodic reactions were hindered strongly and the cathodic reactions were held back slightly. The D-sodium gluconate might behave as a mixed-type inhibitor, but its influence on the anodic processes was dominant. These variations of potentiodynamic polarization curves were likely to be related to the protective film formed by the adsorption of D-sodium gluconate on the steel surface so as to impede the reinforcing steel corrosion in SPS containing 0.1 M NaCl.

The corrosion potentials obtained from the potentiodynamic curves at different immersion times were in good agreement with that obtained from E_{corr} measurements. In the case of the addition of D-sodium gluconate, there were high current density transients appeared in the potentiodynamic polarization curves at the range between -0.080 and 0.010 V. The density current transients had a shape of a quick rise followed by a slow recovery. The typical current density transients indicated the initiation of metastable pitting. The sharp rise of the current was caused by the local breakdown of the adsorptive film. After a short time of pit growth, the repair of the pitted area caused the current to recover to the original value. Therefore, the current density transients directly reflected the initiation, growth and repair processes of metastable pits. Although the metastable pitting occurred, it did not develop to a stable pitting process even after 168 h immersion. The adsorptive film formed by the gluconate anions had some self-repairing capability.

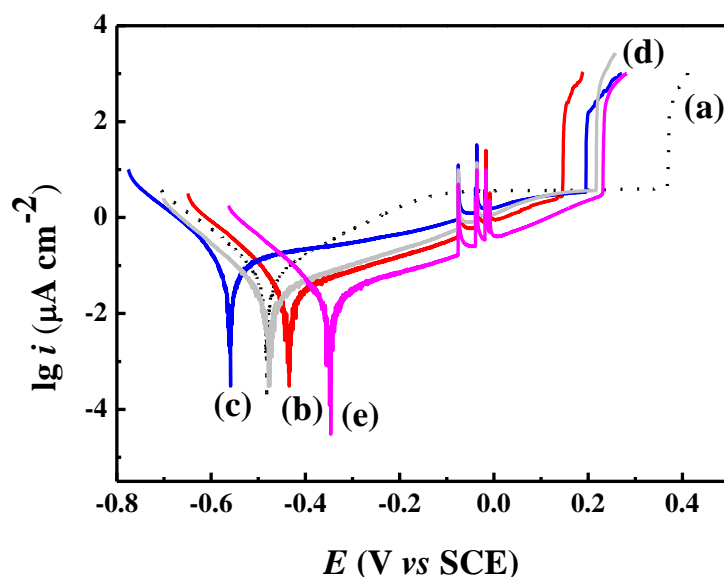


Figure 2. Potentiodynamic polarization curves for the reinforcing steel immersed in SPS containing 0.1 M NaCl (a) without D-sodium gluconate after 1 h immersion and with 0.01 M D-sodium gluconate after different immersion times: (b) 1 h, (c) 12 h, (d) 48 h and (e) 168 h.

3.3. EIS behaviors

The EIS spectra of the reinforcing steel immersed in SPS with 0.1 M NaCl at different immersion times are presented in Figure 3, where Figure 3(a) and (b) are the Bode plots, and Figure 3(c) is the Nyquist plots. On the Bode plots, only one time constant was observed in the low frequency, corresponding to the corrosion process of the reinforcing steel. Moreover, the total impedance decreased gradually with the time and then the large drop was observed for the 36 h immersion. On the Nyquist plots, the semi-circles were observed and the diameter of them decreased during the initial immersion time. The diameter declined significantly for the 36 h immersion. Thereafter, the diameter continued to decrease slowly. The presence of the tail on the plots in Figure 3(a) and (c) indicated the existence of the diffusion process after 36 h of immersion.

The EIS spectra of the reinforcing steel in SPS with 0.1 M NaCl and 0.01 M D-sodium gluconate at different immersion times are shown in Figure 4, where Figure 4 (a) and (b) are the Bode plots, and Figure 4 (c) is the Nyquist plots. The presence of 0.01 M D-sodium gluconate in SPS containing 0.1 M NaCl significantly changed the electrochemical behavior of the reinforcing steel. Only one time constant was observed in the low frequency in Figure 4 (a), which could be related to the interaction of D-sodium gluconate and/or Cl^- with the reinforcing steel surface. The phase angle in the low frequency region reached values close to -90° and phase angle maxima were quite broad in Figure 4 (a), approaching pure capacitive behavior.

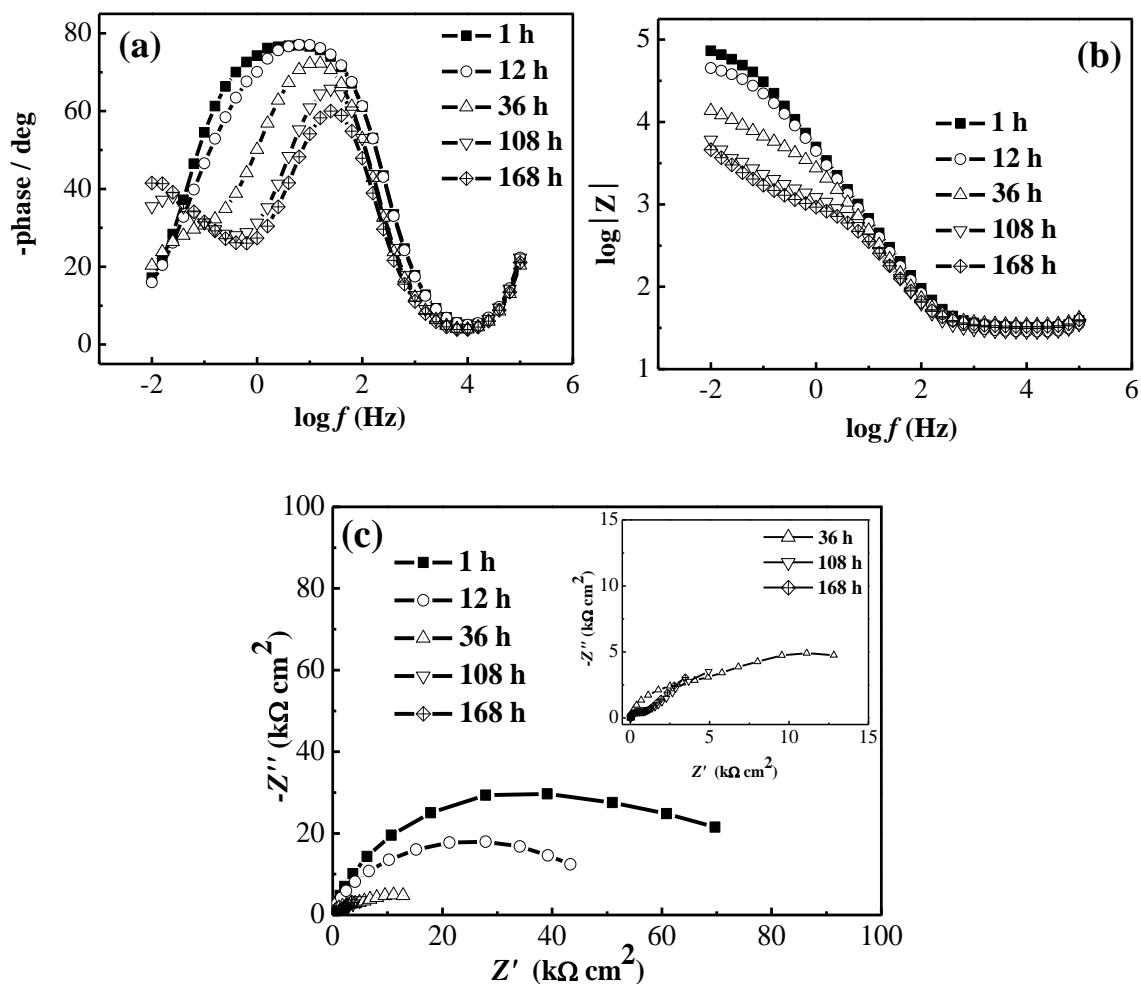


Figure 3. Impedance spectra of the reinforcing steel in SPS with 0.1 M NaCl for different immersion times, (a) and (b) Bode plots, (c) Nyquist plots.

The total impedance showed some fluctuation but no notable change in Figure 4 (b). However, the values of the total impedance were much higher than that without the inhibitor. On Nyquist plots, semi-circles were also observed and the diameter of them changed slightly with immersion time.

The impedance spectra of the reinforcing steel immersed in SPS with 0.1 M NaCl can be described by the equivalent circuit shown in Figure 5, where R_s is the electrolyte resistance, W is the Warburg impedance, R_{ct} is the charge transfer resistance of the corrosion process, and CPE is the constant phase element of the double-layer at the reinforcing steel/electrolyte interface. The Warburg impedance element was added only after 36 h of immersion, corresponding to the oxygen diffusion process. The diffusion of oxygen was slower than the corrosion process and became the control step after 36 h of immersion [46]. With the addition of 0.01 M D-sodium gluconate, the EIS spectra can be fitted by the equivalent circuit shown in Figure 6 during all the immersion time. In Figure 6, R_s is the electrolyte resistance; R_{ct} is the charge transfer resistance and CPE is the corresponding constant phase element, related to the adsorption process of the inhibitor.

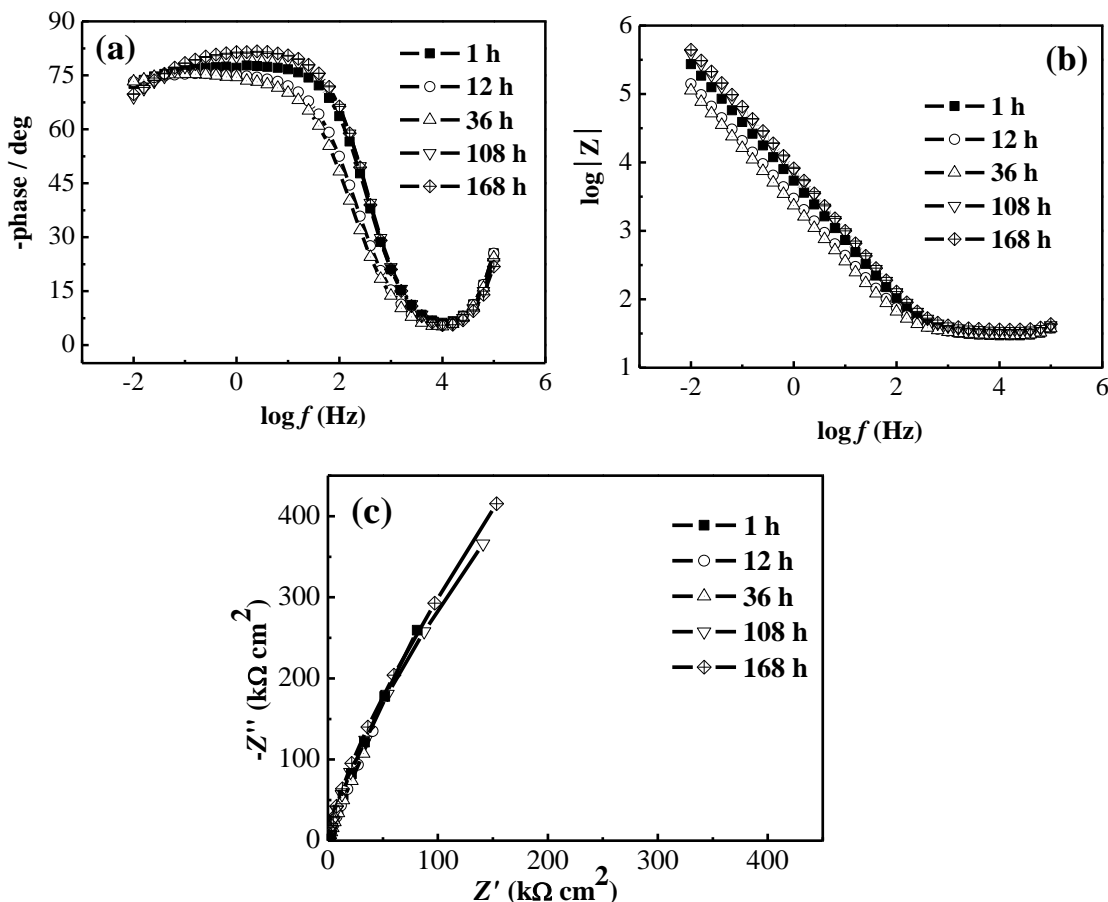


Figure 4. Impedance spectra of the reinforcing steel in SPS with 0.1 M NaCl and 0.01 M D-sodium gluconate for different immersion times, (a) and (b) Bode plots, (c) Nyquist plots.

The CPE is usually interpreted as the non-ideal behavior of the electrochemical interface. Its impedance is defined as follows:

$$Z_{CPE} = Y_0^{-1}(j\omega)^{-n} \quad [1]$$

where Z_{CPE} denotes the impedance of the CPE, Y_0 is a parameter with dimensions of $\Omega^{-1} \text{ cm}^{-2} \text{ s}^n$, which is directly proportional to the double layer capacitance (C_{dl}) of pure capacitive electrodes, ω is the frequency in radians per second, and n is a frequency exponent with values between 0 and 1. When $n = 1$, the CPE can be regarded as the pure capacitance; when $n = 0$, it represents the pure resistance; when $n = 0.5$, it represents Warburg (diffusion) impedance [47-50]. The CPE-parameters Y_0 and n can reflect the change of the electrode surface. A number of studies have shown that the CPE-parameters Y_0 and n varies with the homogeneous of the electrode surface, bigger values of Y_0 and smaller values of n being characteristic of more inhomogeneous surfaces [51-53]. The change of the homogeneous was mainly caused by the electrochemical process occurring on the steel surface in this study. The CPE-parameters Y_0 and n could reflect the initiation and development of the electrochemical process.

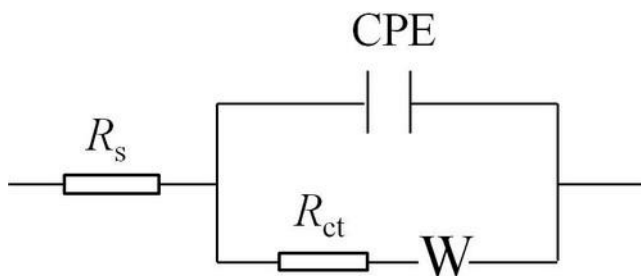


Figure 5. Equivalent circuit for the reinforcing steel immersed in SPS with 0.1 M NaCl.

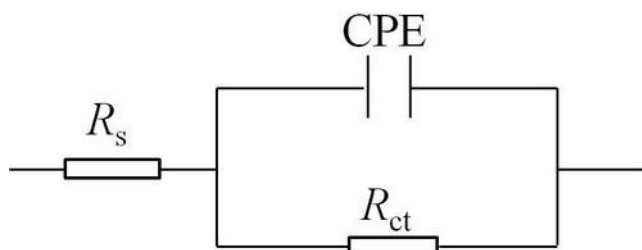


Figure 6. Equivalent circuit for the reinforcing steel immersed in SPS with 0.1 M NaCl and 0.01 M D-sodium gluconate.

The variations of R_{ct} in the presence and absence of 0.01 M D-sodium gluconate in SPS containing 0.1 M NaCl are shown in Figure 7.

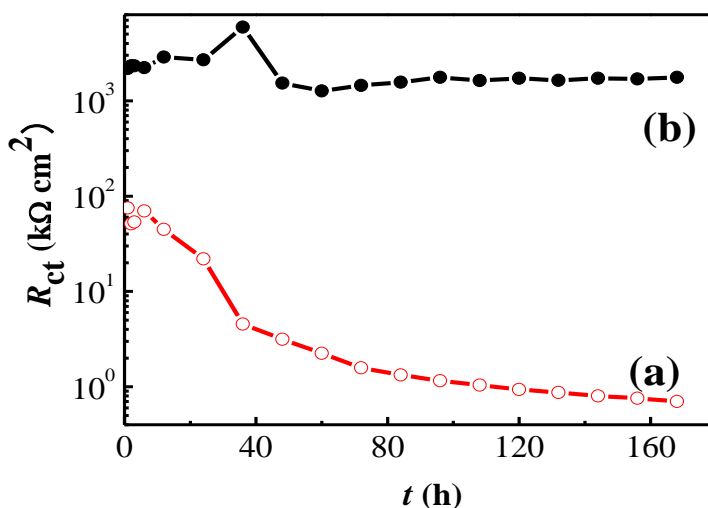


Figure 7. Variation of R_{ct} with time for the reinforcing steel immersed in SPS containing 0.1 M NaCl, (a) without inhibitor, (b) with 0.01 M D-sodium gluconate.

It can be seen that, in the absence of the inhibitor, the R_{ct} value decreased rather quickly during the first 36 h of immersion, and then slowly. After 120 h of immersion, R_{ct} tended to keep stable values (about 1.00 kΩ cm²). The initial large drop of R_{ct} might be caused by the initiation and propagation of

the reinforcing steel corrosion, and then the slow decrease by the severe corrosion under the oxygen diffusion control. However, in the presence of 0.01 M D-sodium gluconate in SPS with 0.1 M NaCl, the R_{ct} change exhibited a very different trend. The R_{ct} value showed a slight increase during the first 36 h of immersion, due to the competitive adsorption between chloride ions and gluconate anions. After that, R_{ct} dropped to the relative low values and then kept almost unchanged (about $1000 \text{ k}\Omega \text{ cm}^2$), indicating the adsorption of D-sodium gluconate and the following formation of an inhibitive film on the reinforcing steel surface. The R_{ct} values in the presence of D-sodium gluconate were much higher than that without the inhibitor during all the immersion time, revealing that D-sodium gluconate had a good corrosion inhibition effect for reinforcing steel in the chloride-contaminated simulated concrete pore solution.

Figure 8 shows the variation of Y_0 in the presence and absence of 0.01 M D-sodium gluconate in SPS containing 0.1 M NaCl. Without D-sodium gluconate, the Y_0 value increased with time during the first 24 h and then was basically stable, indicating the initiation and development of the steel corrosion induced by Cl^- . However, with the addition of 0.01 M D-sodium gluconate, the variation of Y_0 showed a completely different trend. During the initial 36 h of immersion, the Y_0 value largely increased with time due to the competitive adsorption between chloride ions and gluconate anions on the steel surface. Then the Y_0 value began to decrease significantly. After about 132 h of immersion, the Y_0 value kept almost unchanged, suggesting that a protective layer was formed on the steel surface due to the adsorption of gluconate anions on the steel surface. The values of Y_0 for the reinforcing steel in SPS containing 0.1 M NaCl with D-sodium gluconate were higher for the initial 60 h immersion and became lower than that without the inhibitor after 72 h immersion. The change of the Y_0 value reflected the inhibition process of D-sodium gluconate.

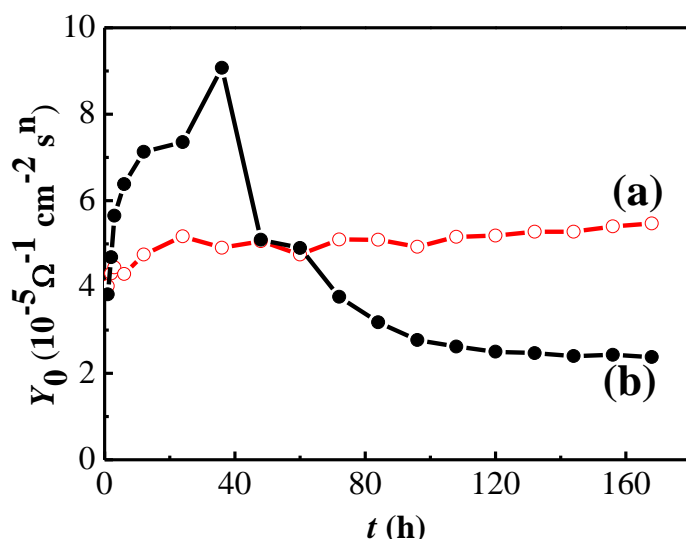


Figure 8. Variation of Y_0 with time for the reinforcing steel immersed in SPS containing 0.1 M NaCl, (a) without inhibitor, (b) with 0.01 M D-sodium gluconate.

Figure 9 depicts the variation of n with time for the reinforcing steel in SPS containing 0.1 M NaCl with and without 0.01 M D-sodium gluconate addition. In the presence and absence of 0.01 M

D-sodium gluconate, the n values all showed the almost opposite change trends as that of the Y_0 values. Therefore, the variations of n also reflected the same inhibition process of D-sodium gluconate on the steel surface.

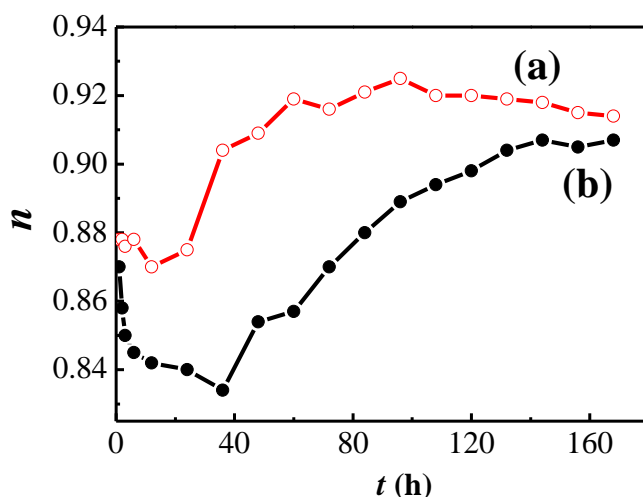


Figure 9. Variation of n with time for the reinforcing steel immersed in SPS containing 0.1 M NaCl, (a) without inhibitor, (b) with 0.01 M D-sodium gluconate.

3.4. Inhibition mechanism of D-sodium gluconate

The changes of all the parameters (R_{ct} , n , E_{corr} and Y_0) obtained from electrochemical measurements showed good agreement with each other. Three stages of the inhibition process of D-sodium gluconate could be distinguished from the variations of these parameters with immersion time. Obviously, there was a critical transition time between the 24 h and 48 h immersion for all parameters. The first stage ranged from the beginning to the time of the critical transition. The second stage started from the critical time to the 132 h of immersion, and the last stage began after 132 h immersion. The scheme of these three stages is illustrated in Figure 10. The first stage might correspond to the competitive adsorption between the gluconate anions and chloride ions on the reinforcing steel surface, resulting in the increase of R_{ct} and Y_0 , and the decrease of E_{corr} and n . At the second stage, the adsorption of gluconate anions became the dominant process, while the adsorption of Cl^- was suppressed and becomes weaker. The gluconate anions might be adsorbed more easily and firmly on the active sites of the reinforcing steel surface, which blocked the adsorption of Cl^- . With time, more gluconate anions were adsorbed on the steel surface, and the adsorptive film formed by gluconate anions was developing on the steel surface, inducing the increase of n and the decrease of Y_0 values. The changes of E_{corr} and R_{ct} also reflected this process. The final stage was related to the formation of a protective film of gluconate anions on the steel surface. In this stage, gluconate anions were adsorbed onto the reinforcing steel surface and formed a compact adsorptive film, meanwhile, the adsorption of Cl^- was inhibited. The adsorptive film exhibited a good barrier effect and could be reflected in the little changes of all the parameters. Therefore, the evolution of all the parameters during the investigation period indicated that the D-sodium gluconate retarded the reinforcing steel corrosion primarily through

the adsorption of gluconate anions and the following formation of a compact adsorptive film on the reinforcing steel surface.

As mentioned above, the corrosion inhibition mechanism of D-sodium gluconate could be based on the adsorption of gluconate anions and then the protective film formed on the reinforcing steel surface. The strong adsorption gluconate anions were mainly due to the chelation. From the structural formula of D-sodium gluconate shown in Figure 11, it can be seen that the gluconate anion contains functional groups ($-\text{COO}^-$ and $-\text{OH}$), which could bond with iron atoms or ions, suggesting that surface chelate formation might occur [36]. Therefore, gluconate anions could be adsorbed onto the reinforcing steel surface. The chelation could strongly enhance the adsorption of gluconate anions on the steel surface, and significantly suppressed the adsorption of Cl^- . The adsorption of gluconate anions eventually formed an adherent and compact protective film on the steel surface, strengthening the corrosion inhibition and retarding the destructive action of Cl^- .

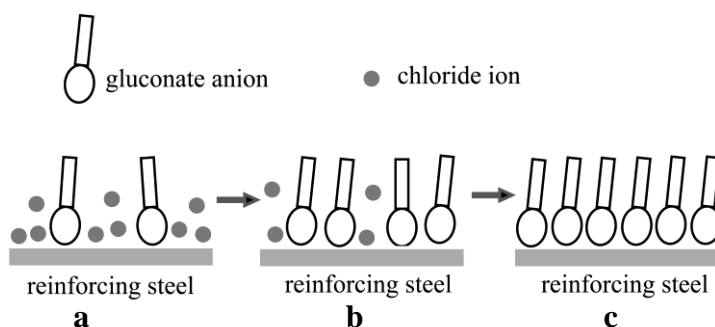


Figure 10. Scheme of three stages of inhibition process of gluconate, (a) the first, (b) the second and (c) the third stage.

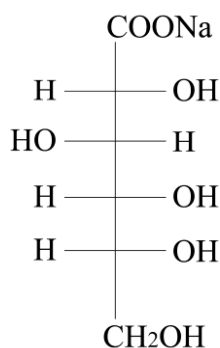


Figure 11. The structural formula of D-sodium gluconate.

4. CONCLUSIONS

The corrosion inhibition effect of D-sodium gluconate on reinforcing steel in SPS with 0.1 M NaCl has been studied by electrochemical techniques. The EIS results were in good agreement with the corrosion potential and potentiodynamic polarization measurements. The results indicated that D-sodium gluconate had a good corrosion inhibition effect on the reinforcing steel in SPS with Cl⁻. Therefore, D-sodium gluconate may be used as a good candidate inhibitor applied in concrete for protecting reinforcing steel from corrosion. D-sodium gluconate effectively inhibited the initiation of reinforcing steel corrosion mainly by suppressing the anodic reaction. The inhibition mechanism could be explained based on the competitive adsorption between gluconate anions and chloride ions on the reinforcing steel surface. Gluconate anions could be adsorbed onto the reinforcing steel surface and finally formed a compact adsorptive film by strong chelation, effectively retarding the Cl⁻ attack.

ACKNOWLEDGEMENTS

This work was supported by the National Natural Science Foundation of China (Nos. 20473066, 21073151, 21173177, J1310024, 21203158).

References

1. A. M. Aguirre, de Gutierrez, R. M. *Mater. Constr.*, 63 (2013) 7.
2. K. Thangavel, *Corros. Rev.*, 22 (2004) 55.
3. V. Kumar, *Corros. Rev.*, 16 (1998) 317.
4. K. Y. Ann, H. W. Song, *Corros. Sci.*, 49, (2007) 4113.
5. A. A. Sagues, A. N. Sanchez, K. Lau, S. C. Kranc, *Corrosion*, 70 (2014) 942.
6. Y. Guo, X. P. Wang, Y. F. Zhu, J. Zhang, Y. B. Gao, Z. Y. Yang, R. G. Du, C. J. Lin, *Int. J. Electrochem. Sci.*, 8 (2013) 12769.
7. H. Xu, Y. Liu, W. Chen, R. G. Du, C. J. Lin, *Electrochim. Acta*, 54 (2009) 4067
8. B. Huet, V. L'Hostis, F. Miserque, H. Idrissi, *Electrochim. Acta*, 51 (2005) 172.
9. R. G. Du, R. G. Hu, R. S. Huang, C. J. Lin, *Anal. Chem.*, 78 (2006) 3179.
10. E. A. H. Al Zubaidy, A. Al Tamimi, *Int. J. Electrochem. Sci.*, 7 (2012) 6472.
11. S. M. Abd El Haleem, S. Abd El Wanees, A. Bahgat, *Corr. Sci.*, 87(2014)321.
12. N. Holmes, R. O'Brien, P. A. M. Basheer, *Mater. Struct.*, 47 (2014) 1531.
13. I. Fayala, L. Dhoubi, X. R. Novoa, M. Ben Ouezdou, *Cem. Concr. Compos.*, 35 (2013) 181.
14. A. Douche-Portanguen, W. Prince, B. Malric, G. Arliguie, *Cem. Concr. Res.*, 35 (2005) 1714.
15. G. K. Glass, A.M. Hassanein, N. R. Buenfeld, *Corros. Sci.* 43 (2001) 1111.
16. R. B. Polder, G. Leegwater, D. Worm, W. Courage, *Cem. Concr. Compos.*, 47 (2014) 69.
17. M. M. S. Cheung, C. Cao, *Constr. Build. Mater.*, 45 (2013) 199.
18. J. M. Miranda, J.A. Gonzalez, A. Cobo, E. Otero, *Corros. Sci.*, 48 (2006) 2172.
19. G. K. Glass, N. R. Buenfeld, *Corros. Sci.*, 42 (2000) 923.
20. T. R. Huang, X. J. Huang, P. C. Wu, *Int. J. Electrochem. Sci.*, 9 (2014) 4589.
21. D. G. Manning, *Constr. Build. Mater.*, 10 (1996) 349.
22. S. Erdogdu, T.W. Bremner, I.L. Kondratova, *Cem. Concr. Res.*, 31 (2001) 861.
23. A. Bautista, J.A. González, *Cem. Concr. Res.*, 26 (1996) 215.
24. N. Gowripalan, H.M. Mohamed, *Cem. Concr. Res.*, 28 (1998) 1119.
25. C. M. Hansson, L. Mammoliti, B. B. Hope, *Cem. Concr. Res.*, 28 (1998) 1775.
26. N. S. Berke, M. C. Hicks, *Cem. Concr. Compos.*, 26 (2004) 191.

27. K. Y. Ann, H. S. Jung, H. S. Kim, S. S. Kim, H. Y. Moon, *Cem. Concr. Res.*, 36 (2006) 530.
28. C. Andrade, C. Alonso, M. Acha, B. Malric, *Cem. Concr. Res.*, 22 (1992) 869.
29. V. T. Ngala, C. L. Page, M. M. Page, *Corros. Sci.*, 45 (2003) 1523.
30. T. Chaussadent, W. Nobel-Pujol, F. Farcas, I. Mabile, C. Fiaud, *Cem. Concr. Res.*, 36 (2006) 556.
31. H. E. Jamil, M. F. Montemor, R. Boulif, A. Shriiri, M.G.S. Ferreira, *Electrochim. Acta*, 48 (2003) 3509.
32. H. E. Jamil, A. Shriiri, R. Boulif, C. Bastos, M.F. Montemor, M.G.S. Ferreira, *Electrochim. Acta*, 49 (2004) 2753.
33. F. Wombacher, U. Maeder, B. Marazzani, *Cem. Concr. Compos.*, 26 (2004) 209.
34. C. Monticelli, A. Frignani, G. TrabANELLI, *Cem. Concr. Res.*, 30 (2000) 635.
35. L. Holloway, K. Nairn, M. Forsyth, *Cem. Concr. Res.*, 34 (2004) 1435.
36. C.K. Nmai, *Cem. Concr. Compos.*, 26 (2004) 199.
37. M. Ormellese, M. Berra, F. Bolzoni, T. Pastore, *Cem. Concr. Res.*, 36 (2006) 536.
38. S. Rajendran, B. V. Apparao, N. Palaniswamy, *Br. Corros. J.*, 33 (1998) 315.
39. O. Lahodny-Sarc, F. Kapor, R. Halle, *Mater. Corros.* 51 (2000) 147.
40. O. Lahodny-Sarc, F. Kapor, *Mater. Corros.*, 53 (2002) 264.
41. S. M. A. Shibli, V. A. Kumary, *Anti-Corros. Methods Mater.*, 51 (2004) 277.
42. S. A. Abd El-Maksoud, S.M. Rashwan, M.A. Ibrahim, S.M. Abd El-Wahaab, *Electrochim. Acta*, 50 (2005) 1985.
43. S. A. M. Refaey, *Appl. Surf. Sci.*, 157 (2000) 199.
44. D. A. Lopez, S. N. Simison, S.R. de Sanchez, *Electrochim. Acta*, 48 (2003) 845.
45. M. A. Amin, S. S. A. El Rehim, E.E.F. El Sherbini, *Electrochim. Acta*, 51 (2006) 4754.
46. A. Prokopowicz, M. Opallo, *Solid State Ion.*, 157 (2003) 209.
47. A. A. Sagüés, S. C. Kranc, E.I. Moreno, *Corros. Sci.*, 37 (1995) 1097.
48. A. A. Sagüés, S. C. Kranc, E. I. Moreno, *Electrochim. Acta*, 41 (1996) 1239.
49. F. Berthier, J. P. Diard, R. Michel, *J. Electroanal. Chem.*, 510 (2001) 1.
50. R. S. Neves, E. De Robertis, A.J. Motheo, *Electrochim. Acta*, 51 (2006) 1215.
51. U. Rammelt, G. Reinhard, *Electrochim. Acta*, 35 (1990) 1045.
52. M. Leibig, T. C. Halsey, *Electrochim. Acta*, 38 (1993) 1985.
53. A. V. Benedetti, P. T. A. Sumodjo, K. Nobe, P. L. Cabot, W. G. Proud, *Electrochim. Acta*, 40 (1995) 2657.